Engineering Journal issn: 0125-8281

Article

Detection of Distorted Meat Image for Pork Grading System

Daisy Sarma*, Pakorn Ubolkosold, and Wisarn Patchoo

School of Engineering, Bangkok University, Paholyothin Road, Klong Luang, Pathum Thani, Thailand
*E-mail: sarma.daisy2000@gmail.com (Corresponding author)

Abstract. This paper proposes a method that detects optical distorted areas (aka *bubble*) in pork images. By correctly identifying and discarding the images containing the unwanted bubbles, a significant improvement of pork image classification (or pork grading) in terms of accuracy has been achieved. The proposed bubble detection method relies on a particular set of image pre-processing techniques followed by morphological and region segmentation operations and is designed to attain the highest bubble detection accuracy for the detection of distorted images. Combining the proposed method with a typical pork image classification technique, the overall classification accuracy has been obtained as high as 96%.

Keywords: Image classification, pork grading, meat grading system.

ENGINEERING JOURNAL Volume 24 Issue 5
Received 17 March 2020
Accepted 3 August 2020
Published 30 September 2020
Online at https://engj.org/
DOI:10.4186/ej.2020.24.5.237

DOI:10.4186/ej.2020.24.5.237

1. Introduction

The common measures used by human graders in determining the pork quality are based on color, muscle area and marbling pattern [1-3]. Among these measures, the marbling pattern is considered to be the primary dominating factor of pork grading in several countries [4-6]. Typically, pork grades are determined by human experts who inspect the pattern of intramuscular fat within the exposed region of pork ribeye. In the past years, computer vision system has been commonly used in the meat industries to assist human graders in the inspection and affirmation of meat quality. In general, computer vision-based meat grading is performed by analyzing the marbling patterns of meat image [7-9]. Such analysis is typically carried out by utilizing the image classification techniques.

Generally, image classifications have been done based on the properties collected from various channels such as RGB, grayscale and binary images [7-9]. In [8], the meat classification has been performed by using grayscale input images in conjunction with gray co-occurrence matrix features. The Binary meat image as input dataset has been examined in [9] by using traditional K-Nearest Neighbor (KNN) algorithm to predict the grades of the meat.

It has been shown in [10] that the performance of the image classification depends on factors such as resolution, noise and distribution of intensity in images. Accordingly, the input images have been enhanced to obtain the higher accuracy. Also, the image quality has been improved for the classification by various filters [11]. In the biomedical applications, the detection of tumors has been performed for the improvement of classification by enhancing the input images [12].

In this paper, the dominant focus is on pork image classification based on the clean image dataset (Fig. 1(a)), where input images have been captured on the top of the photocopy machine. During the capturing, the appearance of bubbles can be attributed to the lighting effects as it fails to attach to the entire area of the meat samples on the given surface (shown in Fig. 1(b)).

In order to improve the performance of pork image classification, it is essential to filter out the bubble images from the dataset. Similarly, the detection of unwanted region has been applied in leaf images to detect the disease [13]. Also, the abnormality detection in medical images has been carried out, and the images have been classified by KNN classifier after detection of unwanted tumor regions [14].

The main objective of this study is to detect and subsequently remove the bubble images, as well as to prevent the new bubble image from appearing in dataset, in order to improve the performance of classification. Figure 2 explains the process of pork image classification for learning and inferring with the classifier based on marbling patterns of the pork meat. The overall classification of pork image and the evaluation of bubble detection method with the classification performance has been explained in following sections.

(a) Clean pork image

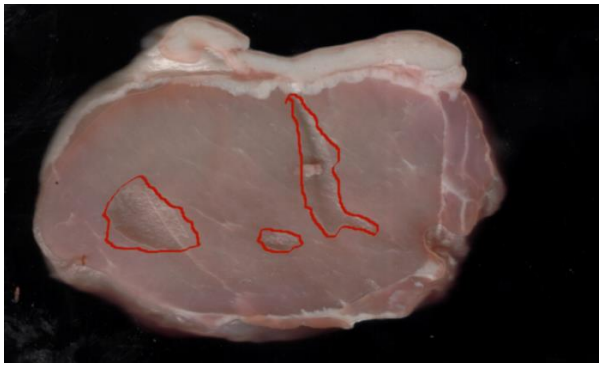

(b) Pork image with bubbles

Fig. 1. Pork images from data set, (a) clean input image, (b) bubble image (optically distorted image).

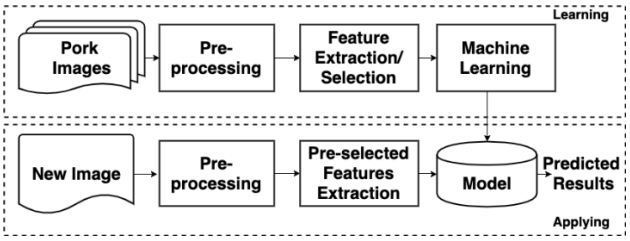

Fig. 2. Block diagram of pork grading system.

2. Proposed Solution

As previously stated, the unwanted bubbles occur during the active process of image capturing due to the lighting effects, when the entire surface of the pork meat sample is not in touch with the surface of the photocopy machine. If the classifier is trained with a dataset that contains bubble images, the low accuracies have been observed. Therefore, it is then proposed to automatically detect and discard the bubble images for better pork grading system (Fig. 3). Bubble detection method has been integrated with mainly pork image classification for the detection and interception of unwanted bubble images. Overall pork grading system involves proposed bubble detection method, data pre-processing and pork image classification which has been explained in the subsequent sections.

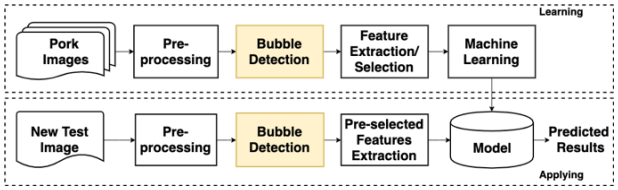

Fig. 3. Proposed grading system with bubble detection.

2.1. Data Pre-processing

Pork images have been labeled with seven grades and used as input dataset for training of the classifier. Four hundred thirty-nine images have been used to perform the feature-extraction of pork images. Number of images in each grade is different, resulting in an imbalanced dataset problem. Therefore, the well-known Synthetic Minority Oversampling Technique (SMOTE) [15-16] algorithm has been applied (see Fig. 4(a, b)) to handle the imbalanced dataset problem. Instead of creating copies, the algorithm works by creating synthetic samples from the minor class with the help of nearest neighbor distances.

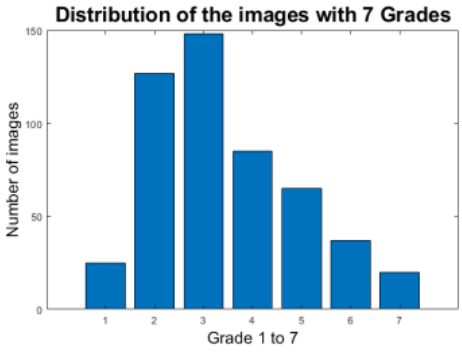

(a) Imbalanced dataset.

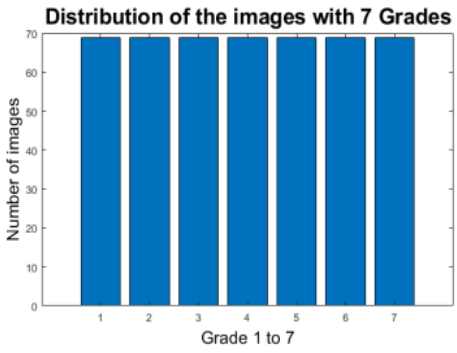

(b) Balanced dataset.

Fig. 4. Distribution of the images per class before/after SMOTE, (a) Imbalanced dataset, (b) balanced dataset.

2.2. Bubble Detection Technique

In this section, the proposed method has been elucidated to further explain the detection of bubbles in pork images before training classifier. After detecting bubbles in pork images, the bubble images are entirely discarded from dataset to increase the accuracy of classification as compared to previous result where the bubble images were in dataset. After pre-processing of cropped pork image, Otsu thresholding [17] has been applied to binarize the image with threshold value between 0 and 1. Edge detection via Sobel kernel has been utilized to smoothen the edges of object in images [18] for detection. Sobel edge detector works using convolution operation and second derivative of image pixel values based on a 3x3 array that is moved over original images to obtain enhanced edges of the object. Binary image noise has been reduced by applying the median filter [19] for furthering the bubble detection. After reducing the noise, morphological operations have been performed to segment the bubbles [20-21] in images. As part of the morphological operations, opening, closing, removal of small blobs and holes filling techniques have been used in the binary images. Morphological operations were applied with disk shape structuring element and radius 15. Using the bounding box (BB) method [20-21], the bubbles have been detected in specific images from image dataset. The largest blob extraction and BB detection has been implemented before classification. If number of BB is greater than zero, then it removes image automatically from the dataset. The highest accuracy of the bubble detection method has been observed at 97%. The process of bubble detection has been shown in Fig. 5 as an example.

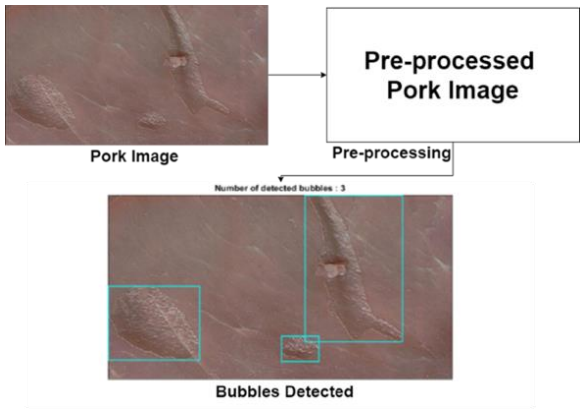

Fig. 5. An example of the bubble detection process.

The steps involved in the proposed method have been enumerated below (Fig. 6),

- Pork image intended for classification is loaded.
- Pork image is cropped in center.
- RGB to L*a*b conversion applied.
- L*a*b to grayscale via PCA performed.
- Otsu thresholding binarization is applied.
- Sobel edge detection technique for the further work.
- Median filtering is used.
- Morphological operations are then performed.
- BB is applied in bubbles.
- Number of BB is counted.

- If the bubbles are detected in image then remove the image from dataset.
- If no bubble detected in image then features has been extracted/selected for classification.
- Classification of the image is carried out.

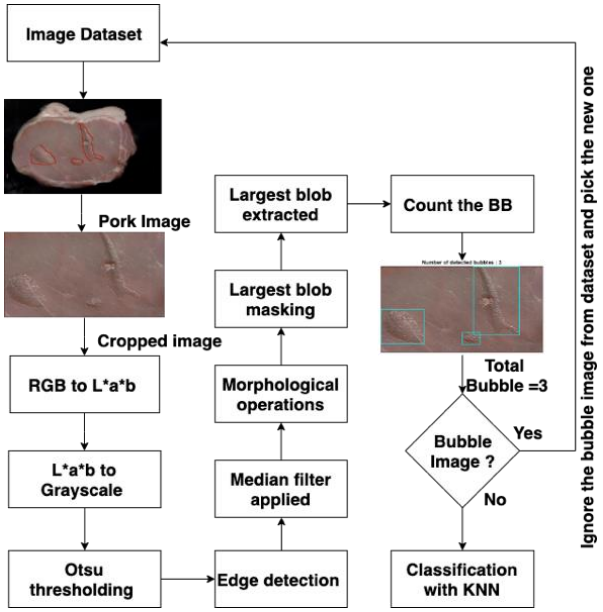

Fig. 6. Flowchart of bubble detection method.

2.3. Image Classification

The pork grading system relies on the KNN-based classification where the image pre-processing, feature extraction and KNN classification techniques have been addressed. The input images have been captured with black backgrounds and have been cropped in center mostly with size (1434 x 820). The classification is comprised of two parts, the training and inferring with the model. The traditional KNN [22-24] has been used as the main classifier. Initially, the input pork images have been smoothened by using Laplacian sharpening [25]. The sharpening work in images is based on the filter coefficients and the sum of the products of co-efficient. Input images have been transformed from RGB to L*a*b color space [26]. Then the L*a*b color space to grayscale conversion via Principle Component Analysis (PCA) [27] technique has been performed to extract the required texture features.

2.4. Feature Extraction Methods

The histogram, co-occurrence and run-length based features have been extracted from grayscale pork images for evaluation of classifier (Table 1). Features have been selected manually based on the observed performance of classifier [28]. First, second and higher order features are also known as histogram [29-30], co-occurrence [31-33], run length-based [34] features set.

From the image histogram, let x is a variable for denoting pork image grey levels and number of grey levels for every count to generate the image histogram is $P(x_n)$, where $n = 0, 1, \cdots, N+1$ be the grayscale histogram and N is the number of distinct grey levels. Mean and energy represents histogram-based feature. Histogram features have been derived basically from (A-1 to A-2) as shown in Table 1.

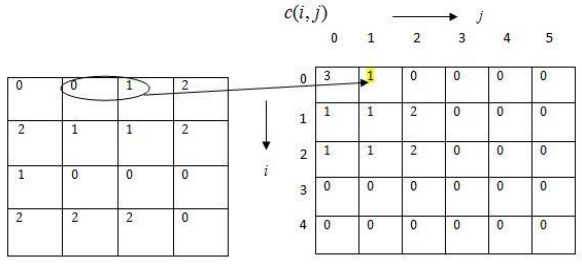

(a) Co-occurrence matrix.

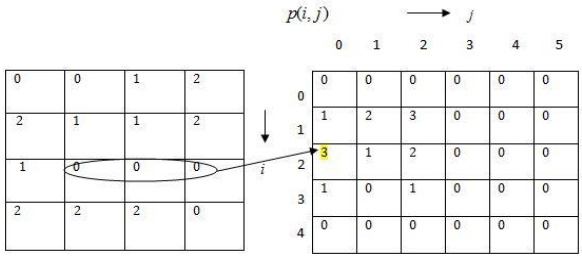

(b) Run-length matrix.

Fig. 7. Example of the co-occurrence and run-length matrix.

Grey level matrix depends on the two neighbor pixel values and direction of values in image. Figure 7(a) is an example of gray level image matrix and the co-occurrence matrix with 0-degree scanning direction. Here, $c(i,j)$ defines the co-occurrence matrix, where i and j are the corresponding neighboring grey levels for row and column. Correlation, inertia, homogeneity, contrast and entropy have been extracted from the grey level co-occurrence matrix (A-3 to A-7) as displayed in equations (see in Table 1), where u and ∂^2 represents the mean and variance of co-occurrence matrix.

In order to calculate the higher order statistics, the run-length matrix has been constructed from gray level image matrix. From the run-length matrix, features have been extracted namely short run emphasis (SRE), long run emphasis (LRE), gray level non-uniformity (GLN) and long run low grey level emphasis (LRLGE) as shown in Table 1 (A-8 to A-11). Figure 7(b) represents a grey level matrix where the run-length matrix has been computed by using 0-degree scanning direction. The $p(i, j)$ defines the run-length matrix, where i and j are grey level and number of run correspondingly and M, N are the total number of distinct grey levels of row and column. The patterns that can be obtained from typical co-occurrence and run-length matrix are highlighted in Fig. 7(a, b) with the yellow color as an example.

Table 1. Features formula.

Mean	$\sum_{n=1}^{N} x_n p(x_n)$	A-1
Energy	$\sum_{n=1}^{N} [p(x_n)]^2$	A-2
Correlation	$\sum_{i,j} \frac{(i-u)(j-u)c(i,j)}{\sigma^2}$	A-3
Inertia	$\sum_{i,j} (i-j)^2 c(i,j)$	A-4
Homogeneity	$\sum_{i,j} \frac{1}{1+\lvert i-j \rvert} c(i,j)$	A-5
Contrast	$\sum_{i,j} \lvert i-u \rvert^2 c(i,j)$	A-6
Entropy	$\sum_{i,j} c(i,j) \log_2 c(i,j)$	A-7
SRE	$\frac{1}{n} \sum_{i=1}^{M} \sum_{j=1}^{N} \frac{p(i,j)}{j^2}$	A-8
LRE	$\frac{1}{n} \sum_{i=1}^{M} \sum_{j=1}^{N} p(i,j) * j^2$	A-9
GLN	$\frac{1}{n} \sum_{i=1}^{M} \left(\sum_{j=1}^{N} \frac{p(i,j)}{i^2} \right)^2$	A-10
LRLGE	$\frac{1}{n} \sum_{i=1}^{M} \sum_{j=1}^{N} \frac{p(i,j) * j^2}{i^2}$	A-11

3. Experimental Process

For the development of pork grading system with the proposed method have been divided in two sections such as bubble detection and pork image classification. After applying the pre-processing in RGB, the binary images have been considered as an input for the bubble detection method and grayscale images for pork image classification. During the process of bubble detection method, number of bubbles in the particular image have been counted to select bubble images from dataset before classification. Bubble detection method has been validated with two conditions such as "bubble" and "no bubble". If the number of bubbles is more than zero, condition one is validated, and the image is identified as "bubble" class. If bubble is detected in image, the image is removed. If not, then the image has been applied into the KNN classifier as shown in Fig. 8. In classification, KNN algorithm tries to find the maximum number of nearest neighbor and it represents the K values of the classifier. Based on the K values, KNN tries to find the nearest classes to classify the unknown events. The parameters involve in bubble detection method and pork image classification have been explained in the next section for further clarity.

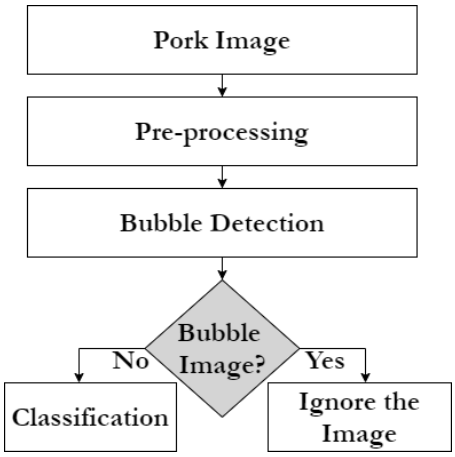

Fig. 8. Pork image classification with bubble detection.

3.1. Experimental Setup

To evaluate the proposed bubble detection, the total number of 439 pork images have been labeled as "bubble" or "no bubble". There are 18 images that contain bubbles. The binarized images are fed in to the proposed detection method. The method then returns the number of bubbles found in images. The overall accuracy of proposed bubble detection method is obtained as the ratio between the correctly detected pork images with and without bubbles and the total number of images. Table 2 shows the features that has been used for pork image classification.

Table 2. Image features for pork grading.

Features	Names
Histogram features	Mean, Energy
Co-occurrence features	Correlation, Homogeneity, Entropy, Contrast and Inertia
Run-length features	SRE, LRE, LRLGE, GLN

To construct co-occurrence and run length matrices from grayscale pork image, the 0 and 90-degree scanning directions have been applied for feature extraction to classify the images. After the feature extraction, image classification has been done based on the selected features with KNN classifier. The K (number of nearest neighbor) value seven has been chosen according to the highest performance of classifier for better pork grading. To evaluate the performance of KNN, the cross-validation has been applied to the pork image dataset with 10 number of folds. The accuracy of classification has been calculated from the confusion matrix.

3.2. Results and Discussion

Table 3 represents the results and comparison of pork image classification which was obtained from histogram, co-occurrence and run length features set.

DOI:10.4186/ej.2020.24.5.237

Table 3. Classification results of each features set.

Cases	Histogram feature set	Co-occurence feature set	Run length Feature set	Accuracy
1	✓	-	-	71%
2	-	✓	-	73%
3	-	-	✓	73%

By using the proposed bubble detection method, the images have been deleted automatically with the highest accuracy of 97% (Fig. 9). Without the bubble detection in pork image classification, the images have been classified as displayed in Fig. 10 with the accuracy as low as 76%. After removing the bubble images from input dataset, the performance of the classifier has been increased as shown in Fig. 11. The results that have been obtained from each steps of bubble detection method are shown in Fig. 12(a-k). The original pork image, center cropped, the RGB to grayscale, Otsu binarized, edge detected, filtered and the bubble image with the detection have been displayed to validate the results of proposed bubble detection method before the classification for pork grading system in Fig. 12(a-k). The accuracies of pork image classification, the detection and the classification with proposed bubble detection method have been obtained from the confusion matrices below by dividing all the diagonal values with the total number of values in these matrices. As a result, the three bubbles have been detected in an image (Fig. 12(k)). With the validation of bubble detection method, the pork image classification accuracy has been increased from 76% to 96% correctly to develop a better pork grading system.

Actual Class ↓ / Predicted Class →	Bubble	No bubble
Bubble	11	7
No bubble	7	414

Fig. 9. Performance matrix of proposed method.

Actual Grade ↓ / Predicted Grade →	1	2	3	4	5	6	7
1	12	2	5	2	0	1	0
2	2	75	10	6	1	1	0
3	1	12	92	8	6	1	0
4	2	1	9	60	5	5	0
5	0	0	4	9	43	2	1
6	0	0	0	1	1	38	1
7	0	0	1	2	2	0	15

Fig. 10. Confusion matrix of pork image classification without bubble detection.

Actual Grade ↓ / Predicted Grade →	1	2	3	4	5	6	7
1	16	2	0	1	0	0	0
2	0	102	3	0	1	0	0
3	0	2	125	0	0	0	0
4	0	1	0	65	1	0	0
5	0	0	2	0	62	1	0
6	0	0	0	0	1	18	0
7	0	0	1	0	1	0	23

Fig. 11. Confusion matrix of pork image classification with proposed bubble detection.

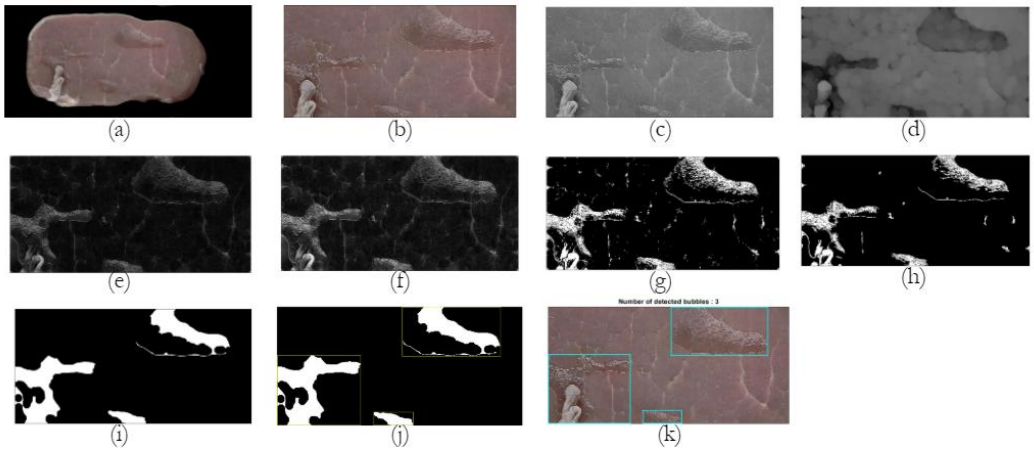

Fig. 12. Results from the proposed method for the pork grading system. (a) Original image, (b) Cropped image, (c) Grayscale image, (d) Dilated image, (e) Edge detected image, (f) Binary image, (g) Filtered image, (h) Remove small blobs, (i) Fill big blobs, (j) Bounding box on big blobs, (k) Bubbles detected successfully in RGB cropped image.

4. Conclusion

Bubble detection method has been shown to be capable of removing the bubble images from dataset with 97% accuracy. By detecting the bubble images from dataset, the accuracy of pork image classification with KNN algorithm has been improved from 76% to 96%.

Bubble detection method can also be applied for same kind of distorted images in different applications such as biomedical, food and agriculture.

Acknowledgement

This research was supported by ECE Graduate Program, Bangkok University. We are also thankful to Dr. Supamit Mekchay from Chiang Mai University who provided us with the pork images that greatly assisted our research.

References

[1] J. Xing, M. Ngadi, A. Gunenc, S. Prasher, and C. Gariepy, "Use of visible spectroscopy for quality classification of intact pork meat," *Elsevier Journal of Food Engineering*, vol. 82, no. 2, pp. 135–141, 2007.

[2] P. Jackman, D.-W, Sun, P. Allen, N. A. Valous, F. Mendoza, and P. Ward, "Identification of important image features for pork and turkey ham classification using color and wavelet texture features and genetic selection," *Elsevier Meat Science*, vol. 84, no. 4, pp. 711–717, 2010.

[3] M. Zheng, Y. Huang, J. Ji, S. Xiao, J. Ma, and L. Huang, "Effects of breeds, tissues and genders on purine contents in pork and the relationships between purine content and other meat quality traits," *Elsevier Meat Science*, vol. 143, pp. 8186, 2018.

[4] L. Faucitano, P. Huff, F. Teuscher, C. Gariepy, and J. Wegner, "Application of computer image analysis to measure pork marbling characteristics," *Elsevier Meat Science*, vol. 69, pp. 537-543, 2005.

[5] W. Cheng , J.-H. Cheng, D.-W. Sun, and H. Pu, "Marbling analysis for evaluating meat quality: Methods and techniques," *Comprehensive Reviews in Food Science and Food Safety*, vol. 14, pp. 523–535, 2015.

[6] H. Huang, L. Liu, M. O. Ngadi, and C. Gariepy, "Prediction of pork marbling scores using pattern analysis techniques," *Elsevier Food Control*, vol. 3, no. 1, pp. 224–229, 2013.

[7] J. Lu, P. Shatadal, and D. Gerrard, "Evaluation of pork color by using computer vision," Elsevier Meat Science, vol. 56, pp. 57–60, 2000.

[8] K. Shiranita, T. Miyajima, and R. Takiyama, "Determination of meat quality by texture analysis," *Elsevier Pattern Recognition*, vol. 19, pp. 1319–1324, 1998.

[9] A. P. A. da Costa Barbon, S. Barbon Jr., G. F. C. Campos, J. L. Seixas Jr., L. M. Peres, S. M. Mastelini, N. Andreo, A. Ulirici, and A. M. Bridi, "Development of a flexible Computer Vision System for marbling classification," *Elsevier Computers and Electronics in Agriculture,* vol. 142, pp. 536–544, 2017.

[10] M. Koziarski and B. Cyganek, "Impact of low resolution on image recognition with deep neural networks: An experimental study," *International Journal of Applied Mathematics and Computer Science*, vol. 28, no. 4, pp. 735–744, 2018.

[11] R. Ramani, Dr. N. Suthanthira Vanitha, and S. Valarmathy, "The pre-processing techniques for breast cancer detection in mammography images," *I. J. Image Graphics and Signal Processing*, vol. 5, pp. 47–54, 2013.

[12] Y.. A. Labeeb, M. Morsy, and M. E. A. Abo-Elsoud, "Preprocessing technique for the enhancement of the dicom kidney images," *IJRASET*, vol. 3, pp. 836–841, 2015.

[13] K. R. Gavhale, U. Gawande, and K. O. Hajari, "Unhealthy region of citrus leaf detection using image processing techniques," in *International Conference for Convergence for Technology*, 2014, pp. 1–6.

[14] R. J. Ramteke and K. Y. Monali, "Automatic medical image classification and abnormality detection using k- nearest neighbor," *International Journal of Advanced Computer Research*, vol. 2, no. 4, pp. 190–196, 2012.

[15] N. V. Chawla, K. W. Bowyer, L. O. Hall, and W. P. K. Meyer, "SMOTE: Synthetic Minority Over-sampling Technique," *Journal of Artificial Intelligence Research*, vol. 16, pp. 321–357, 2002.

[16] Q. Wang, Z. H. Luo, J. C. Huang, Y. H. Feng, and Z. Liu, "A novel ensemble method for imbalanced data learning: Bagging of extrapolation-SMOTE SVM," *Computational Intelligence and Neuroscience*, pp. 1–11, 2017, Article ID 1827016.

[17] P. Puneet and N. Kumar Garg, "Binarization Techniques used for Gray Scale Image," *International Journal of Computer Applications,* vol. 71, pp. 8–11, 2013.

[18] A. Sharma and S. Jaswal, "Analysis of sobel edge detection technique for face recognition," *IJARCET*, vol. 4, no. 5, pp. 2450–2453, 2015.

[19] W. W. Boles, M. Kanefsky, and M. Simaan, "A reduced edge distortion median filtering algorithm for binary images," *Elsevier Signal Processing*, vol. 21, no. 1, pp. 37–47, 1990.

[20] N. B. Bahadure, A. K. Ray, and H. P. Thethi, "Image analysis for MRI based brain tumour detection and feature extraction using biologically inspired BWT and SVM," *International Journal of Biomedical Imaging*, pp. 1–12, 2017.

[21] A. H. M. Zadidul Karim, Md. Abdullah Al Mahmud, M. Abdullah Al Amin, and M. Towhidur Rahman, "Brain tumour detection by using bounding box methodology based on bhattacharyya coefficient," *American Journal of Engineering Research*, vol. 5, no. 12, pp. 218–223, 2016.

[22] T. Cover and P. Hart, "Nearest neighbor pattern classification," *IEEE Transactions on Information Theory*, vol. 13, no. 1, pp. 21–27, 1967.

[23] N. Krithika, and A. Grace Selvarani, "An individual grape leaf disease identification using leaf skeletons and KNN classification," in *IEEE ICIIECS*, India, 2017, pp. 1–3.
[24] S. Augstin and R. Dijaya, "Beef image classification using k-nearest neighbour algorithm for identification quality and freshness," *IOP Journal of Physics: Conference Series*, vol. 1179, 2019.
[25] F. Malik and B. Baharudin, "The statistical quantized histogram texture features analysis for image retrieval based on median and laplacian filters in the DCT domain," *The International Arab Journal of Information Technology*, vol. 10, no. 6, 2013.
[26] K. K. Niranjana and M. Kalpana Devi, "RGB to lab transformation using image segmentation," *IJARCSMS*, vol. 3, pp. 8–16, 2015.
[27] J.-W.Seo and S. D. Kim, "Novel PCA-based color-to-gray image conversion," in *IEEE International Conference on Image Processing*, Melbourne, VIC, 2013, pp. 2279–2283.
[28] I. Guyon and A. Elisseeff, "An introduction to variable and feature selection," *Journal of Machine Learning Research*, vol. 3, pp. 1157–1182, 2003.
[29] Garali, M. Adel, S. Bourennane, and E. Guedj, "Histogram-based features selection and volume of interest ranking for brain PET image classification," *IEEE Journal of Translational Engineering in Health and Medicine*, vol. 6, pp. 1–12, 2018.
[30] A. S. Sinaga, "Texture features extraction of human leather ports based on histogram," *IJAIDM*, vol. 1, no. 2, pp. 86–91, 2018.
[31] A. Suresh, and K. L. Shunmuganathan, "Image texture classification using grey level co-occurrence matrix based statistical features," *European Journal of Scientific Research*, vol. 75, no. 4, pp. 591–597, 2012.
[32] B. Sebastian V., A. Unnikrishnan, and K. Balakrishnan, "Grey level co-occurrence matrices: Generalisation and Some New Features," *International Journal of Computer Science. Engineering and Information Technology*, vol. 2, no. 2, pp. 151–157, 2012.
[33] R. A. Asmara, R. Romario, K. S. Batubulan, E. Rohadi, I. Siradjuddin, F. Ronilaya, R. Ariyanto, C. Rahmad, and F. Rahutomo, "Classification of pork and beef meat images using extraction of color and texture feature by Grey Level Co-Occurrence Matrix method," *Materials Science and Engineering*, vol. 434, pp. 1–10, 2018.
[34] X. Tang, "Texture information in run-length matrices," *IEEE Transaction on Image Processing*, vol. 7, no. 11, 1998.

Appendix

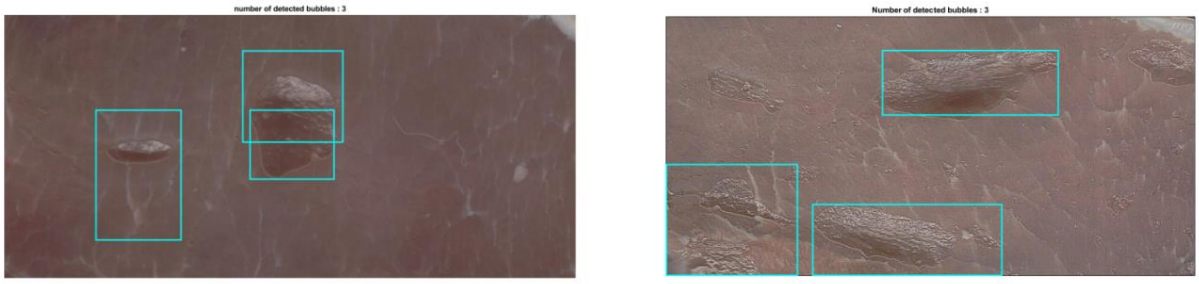

Fig. 13. Results obtained by the buble detection method.

Daisy Sarma, photograph and biography not available at the time of publication.

Pakorn Ubolkosold, photograph and biography not available at the time of publication.

Wisarn Patchoo, photograph and biography not available at the time of publication.